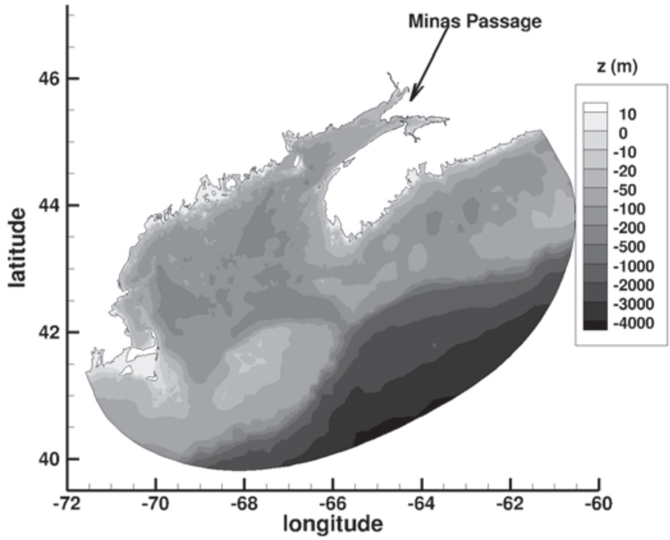

Figure 4: Model domain showing the Bay of Fundy and Minas Passage. The tidal turbines are located in Minas Passage in a line and distributed arrangement.

vertices and 134167 triangular elements. On a desktop computer, the model runs 60 times faster (2D) and 15 times faster (3D) than simulated time. Hence a 34 day run for harmonic analysis takes slightly longer than 12 hours in 2D. This efficiency enables a thorough investigation of flow dynamics by multiple parameter variation.

The model (2D) was run for a 34 day simulation, and the results from a harmonic analysis of the sea level time series was compared to values of amplitude and phase derived from observations at sites ranging from Cape Cod to Minas Basin. From these results, the bottom friction coefficient was set at 0.002 and this data set forms a baseline for later comparisons. Next, the model (3D) was run for 6 different 34 day periods and the velocity profiles in Minas Passage were compared to ADCP current meter observations. This phase of the study provides an assessment of whether the model provides a faithful reproduction of the dynamics of the Bay of Fundy system. Typically, sea level harmonics agreed within a few cm and ^{o} for most of the observation sites. This is considered adequate for the purposes of this study.

Next, form drag representing turbines was added to the model (2D) following the formulation in (16). Although several turbine arrangements were examined, two cases are considered here as indicative of the range of results. The first arrangement is a strip of form drag approximately 200 m wide across the entrance to Minas Passage, which is equivalent to a line of turbines at the entrance. The second arrangement is a uniform form drag over the entire Minas Passage (about 8 km), which is equivalent to a turbine farm distributed evenly over this area. Then the model (2D) was run for 100 hours with increasing values for form drag until the results extend beyond the peak power predicted from the theory of Garrett and Cummins (2004). The results for total power are then averaged between the minima at approximately 72 and 97 hours, thereby eliminating the spinup period. These results are then plotted as average power vs form drag coefficient $c_{fd} = (1/2)C_D\lambda_f$ from eq. 16.

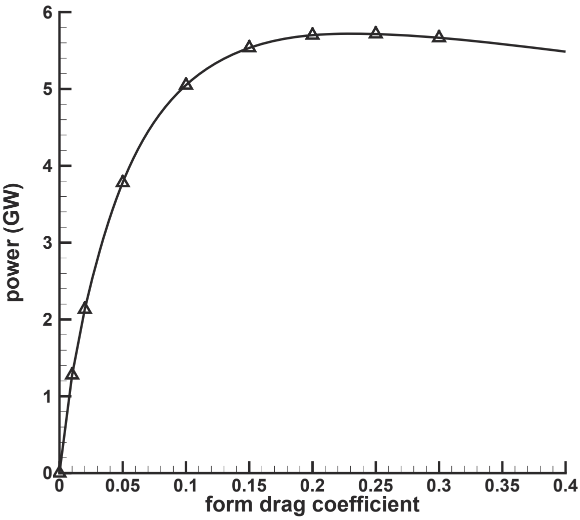

Figure 5: Average power as a function of form drag coefficient c_{fd} for the distributed scenario where $C_D = 1$. For the line scenario, the results are similar with the abscissa multiplied by 42. A line is fit to the data points (symbols).

As predicted by the theory presented in Garrett and Cummins (2004), there is a similar peak value for average power for the line and distributed scenarios. For a given geometry and forcing, the factor rL is constant, where r is a friction coefficient and L is the length of the channel over which the turbines are distributed. Then for large L such as the distributed case, the friction coefficient necessary to attain peak average power is smaller. Otherwise, the theoretical solutions are identical.

However, the main point of the present study is that the value for the friction coefficient (form drag coefficient here) is severely limited for tidal turbine technology. The value for form drag coefficient is given by (2D, see eq. 16)

$$c_{fd} = (1/2)(A_f/A)C_d \tag{17}$$

where C_d is the drag coefficient which is of $O(1)$ (typically between 0.2 and 1.0 for the operating range of tidal turbines). The remaining factor A_f/A represents the frontal area divided by the footprint of a turbine and is determined by the placement and density of the turbines. For a horizontal shaft turbine with a $30m$ diameter impeller that is spaced 3 diameters from its neighbors in the flow direction and 2 diameters in the lateral direction, $A_f = 707m^2$ and $A = 8100m^2$ so that $c_{fd} = 0.04$ assuming $C_d = 1$.

As may be seen in figure 5, the limit on c_{fd} is generally much less than the value where the maximum power is attained. For the line case, maximum power is extracted for $c_{fd} = 8.5$; whereas, for the distributed case, maximum power is extracted for $c_{fd} = 0.2$. These values can be compared to the estimated value for turbines, $c_{fd} = 0.04$.

Example: Tsunami runup

The final example illustrates the use of subgrid refinement following the approach of Casulli (2008) and Casulli and Stelling (2011). The example presented here is for a tsunami generated by a megathrust rupture on the Cascadia plate boundary. Although the computational grid extends from north of Vancouver Island to southern California, the area of interest is the area around Ucluelet, on the west coast of Vancouver Island. The grid is composed of triangular elements with an edge length that varies from approximately $10km$ on the open boundary to $10m$ around Ucluelet. The results for the maximum water elevation is shown in figure (6)

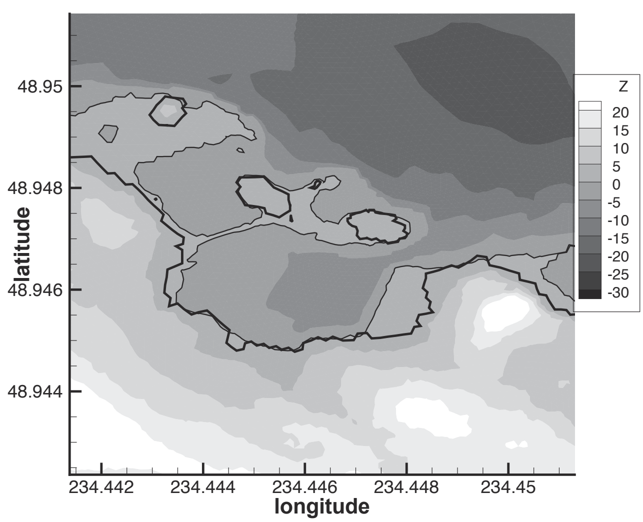

Figure 6: Maximum water elevation (m) at Ucluelet. Heavy line is maximum water elevation, medium line is mean sea level after approximately $2.1m$ subsidence.

For the subgrid calculations, all the elements below $5m$ elevation were replaced by 4^{th} order elements with 5 vertices on each edge. Elevation at the subgrid vertices was interpolated from gridded topography with $1m$ spacing in the horizontal and better than $0.1m$ accuracy in the vertical. The subgrid topography was approximated with piecewise linear functions.

The results for maximum water elevation are similar for both the calculations with subgrids and without subgrids. The most difference in the simulations was during the runup and rundown periods when the area was partially wet. In addition, the area along the waterfront tended to retain water in the simulation without subgrids. The additional drainage channels in the subgrid performed better in this respect.

The original idea with using subgrids was to coarsen the grid and allow the model to run faster. While this could be done in many places such as the west coast beaches, the area around Ucluelet required the $10m$ resolution to properly represent the flow into the harbor. Hence, this was a partial success.

Conclusions

Double-averaging methods (DAM) present a viable approach to approximating subgrid effects in a numerical model. The key issue is forming closures for the averages over the subgrid variations. Fortunately, these can be represented as a form drag term in most cases. The use of subgrids provides methods for approximating the volume and flux integrals while not requiring subgrid velocity calculations. In the case of tsunami runup, an interesting application of these methods would be to use subgrids to capture the topographic details, and use form drag as formulated by DAM to represent vegetation and obstacles in the flow.

References

Casulli, V., 2008. A high-resolution wetting and drying algorithm for free-surface hydrodynamics. Int. J. Numer. Meth. Fluids. DOI:10.1002/fld.1896.

Casulli, V., Stelling, G., 2011. Semi-implicit subgrid modelling of three-dimensional free-surface flows. International Journal for Numerical Methods in Fluids. DOI: 10.1002/fld.2361.

Garrett, C., 1972. Tidal resonance in the Bay of Fundy and Gulf of Maine, Nature 238, 441–443.

Garrett, C., Cummins, P., 2004. Generating power form tidal currents, Journal of Waterway, Port, Coastal, and Ocean Eng. 130, 114–118.

Greenberg, D.A., 1979. A numerical model investigation of tidal phenomena in the Bay of Fundy and Gulf of Maine. Marine Geodesy 2(2), 161–187.

Nikora, V., McLean, S., Coleman, S.,Pokrajac, D., Walters, R., 2007. Double-averaging concept for rough-bed open-channel and overland flows: Theoretical background. J. Hydraul. Eng. ASCE 133, 873-883.

Nikora, V., Rowinski, P., 2008. Preface to Special Issue. Acta Geophysica 56(3), 529-533.

Pasche, E., and G. Rouve, 1985, Overbank flow with vegetatively roughened flood plains, Journal of Hydraulic Engineering 111, 1262-1278.

Pinder, G.F., Gray, W.G., 1977. Finite Elements in Surface and Subsurface Hydrology. Academic Press.

Stone, B.M., and H.T. Shen, 2002, Hydraulic resistance of flow in channels with cylindrical roughness, Journal of Hydraulic Engineering 128(5), 500-506

Sucsy, P.V., Pearce, B.R., Panchang, V.G., 2006. Comparison of two-and three-dimensional model simulation of the effect of a tidal barrier on the Gulf of Maine tides, Journal of Physical Oceanography 23(6), 1231–1248.

Walters, R. A., Gillibrand, P., Bell, R., Lane, E.M., 2010. A study of tides and currents in Cook Strait, New Zealand. Ocean Dynamics 60, 15591580. DOI 10.1007/s10236-010-0353-8

Walters, R.A., Hanert, E., Pietrzak, J.D., Le Roux, D.Y., 2009a. Comparison of unstructured, staggered grid methods for the shallow water equations. Ocean Modelling 28, 106–117.

Walters, R.A., Plew, D.R., 2008. Numerical modelling of environmental flows using DAM: Some preliminary results. Acta Geophysica 56(3), 918–934.

Wu, W., Shields Jr., F. F., Bennett, S. J,. and Wang, S. S. Y., 2005, A depth-averaged two-dimensional model for flow, sediment transport, and bed topography in curved channels with riparian vegetation, Water Resources Research 41, W03015.

Modeling Sediment Disposal in Inshore Waterways of British Columbia, Canada

Jianhua Jiang[1] and David B. Fissel[1]

Abstract

In support of the environmental assessment and regulatory approval process and as an interim guidance for field work, a number of numerical modeling studies of the sediment disposals were recently carried out by ASL Environmental Sciences Inc. at the designated/potential disposal sites in inshore waterways of British Columbia, Canada, using the 3D numerical model COCIRM-SED and the short-term fate model of sediment disposal STFATE. In these applications, STFATE was used to provide initial distributions of suspended sediment and bottom accumulation in details, typically within the first hour of the sediment disposal operation, as a useful interim guidance for field work and input to the 3D model COCIRM-SED, which was then adapted to examine the transport and fate of all disposal materials over much larger spatial scales and longer periods of time. This paper reports the model approaches and the detailed model results in the Brown Passage application.

Introduction

Dredged marine sediment and excavated terrestrial overburden from coastal engineering projects are commonly disposed at designated sites in ocean and coastal open waters via release from barges or pipelines. However, the sediment disposal in these areas can have adverse environmental impacts, especially on marine life and fish habitats, in the form of bottom accumulation and increasing total suspended sediment (TSS) levels in the water column (Fissel and Jiang, 2011). Thus, the short-term (with durations of hours to about a day) and long-term (with durations of days to months) transport and fate of the disposal sediment during and after the disposal operations are of particular concern to coastal engineers and environmental scientists in assessing potential environmental effects and obtaining regulatory approval. The progress realized in advanced circulation and sediment transport numerical models provides useful and reliable tools in quantitatively predicting transport and fate of disposal sediment.

Recently in ASL Environmental Sciences Inc., numerical modeling studies of the short-term and long-term transport and fate of the disposal sediment were successfully carried out at a number of designated/potential sediment disposal sites in the inshore waterways of British Columbia, Canada (Figure 1). These studies used the ASL's own 3D COastal CIRculation and SEDiment transport Model (COCIRM-SED) and the Short-term FATE model of sediment disposal (STFATE), developed by the U.S. Army Corps of Engineers. The model results were used to address the potential impacts of the sediment disposal on the natural environment of receiving ambient

[1]ASL Environmental Sciences Inc., #1 – 6703 Rajpur Place, Victoria, BC, V8M 1Z5, Canada, jjiang@aslenv.com and dfissel@aslenv.com

waters, and to support regulatory approval process as well as provide interim guidance for field work.

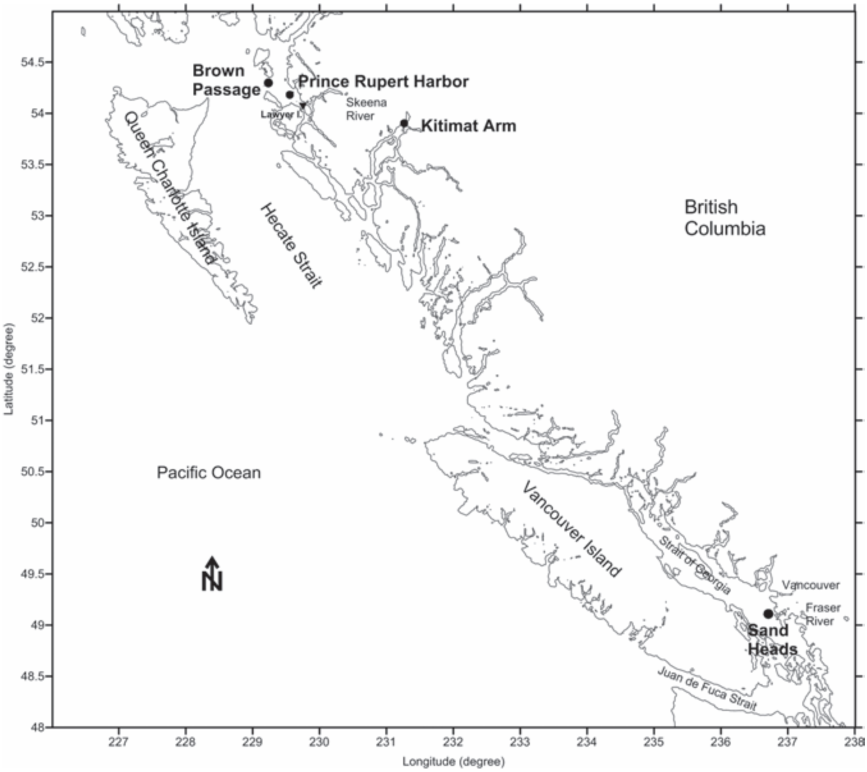

Figure 1. A map showing locations of the sediment disposal sites in the inshore waterways of British Columbia, Canada.

One particular regional ocean disposal site in Brown Passage involves the disposal of dredged marine sediment and possible excavated terrestrial overburden from Prince Rupert Harbor development site via release from barge (Jiang and Fissel, 2010). In this application, STFATE was used to model the initial operation of each disposal trip and to provide detailed input information of initial bottom accumulation and suspended sediment concentration (SSC) in the water column to COCIRM-SED, which then simulated the transport and fate of all disposal sediment as well as potential resuspension over a much larger spatial scale and a longer period of time.

This paper presents the model approaches and the detailed model results in the Brown Passage application, including TSS values above background level, TSS plumes, total bottom accumulation and potential long-term resuspension of the disposal sediment deposited on the seabed.

Model Approach

COCIRM-SED and STFATE Overview

STFATE, developed by the U.S. Army Corps of Engineers, is a short-term fate model of sediment disposal, which is accepted by the U.S. Environmental Protection Agency (EPA and USACE, 1995). The STFATE model was used to simulate the short-term fate and near-field distribution of the disposal material released from the barge immediately following each disposal operation. The STFATE operated on the actual bathymetry using an identical or smaller model mesh to match the 3D model COCIRM-SED grid, and ran over the initial 45 minutes of the disposal operation. During the initial 45 minutes of the disposal operation, the disposal sediment released from the barge underwent the processes of convective descent, horizontal transport under background current, turbulence diffusion, dynamic collapse, and meanwhile, deposition of most coarse sediments with size larger than medium sand. The ocean current input to STFATE included typical tidal stages, such as peak and mean flood and ebb as well as slack water, freshet and dry seasons, and different wind conditions. The STFATE output provided input information to the 3D model COCIRM-SED in detail, including bottom accumulation and suspended sediment concentrations (SSC) and distributions by categories during the initial disposal operation, and COCIRM-SED then simulated the transport and fate of all dredged/excavated materials over much larger spatial scales and longer periods of time.

The 3D coastal circulation numerical model COCIRM-SED, used in these studies, is a highly-integrated, three-dimensional, free-surface, finite-difference numerical model code for use on rivers, lakes, estuaries, bays, coastal areas and seas (Jiang et al., 2003; Jiang and Fissel, 2004; Jiang, et al., 2008; Fissel and Jiang, 2008), and consists of five sub-modules including circulation, multi-category sediment transport, morphodynamics, water quality and particle tracking (Figure 2). All modules operate as subroutines together within the COCIRM-SED model, and the model can be operated on either an integrated or an individual module basis. The model applies the fully three-dimensional primitive equations of motion and conservative mass transport combined with a second order turbulence closure model, then solves for time-dependent, three-dimensional velocities, salinity, temperature, SSC and coarse sediment bed-load transport by size category, turbulence kinetic energy and mixing length, horizontal and vertical diffusivities, water surface elevation, bottom elevation variations, and multiple water contaminant concentrations. It also includes wetting/drying and nested grid schemes, capable of incorporating tidal flats, jet-like outflows, outfall mixing zone and other relatively small interested areas. Horizontal resolution can range from <10 m to a few kilometers, and vertical resolution typically ranges from 10 to 30 layers either as a sigma- or a z-layers coordinate with uneven distribution of layer thickness. In all implementations of simulating sediment disposals, the COCIRM-SED circulation module was validated using historical water level and ocean current data in the model areas.

To activate the sediment transport and morphological modules, one need only input the grain size (d_k) and percentage fraction (f_k) for each sediment category, with typically total category 5 – 20. COCIRM-SED readily simulates settling velocities (w_k), suspended sediment concentration (c_k), bed-load rates ($S_{b,k}$), and bottom elevation changes by size category. For fine-grained sediments with particle size less than 32 – 62 μm (clay – silt range), modeling of cohesive sediment transport will be involved, while for coarse sediments with particle size greater than 32 – 62 μm (sand, granule and fine pebble), modeling of non-cohesive sediment transport will be activated.

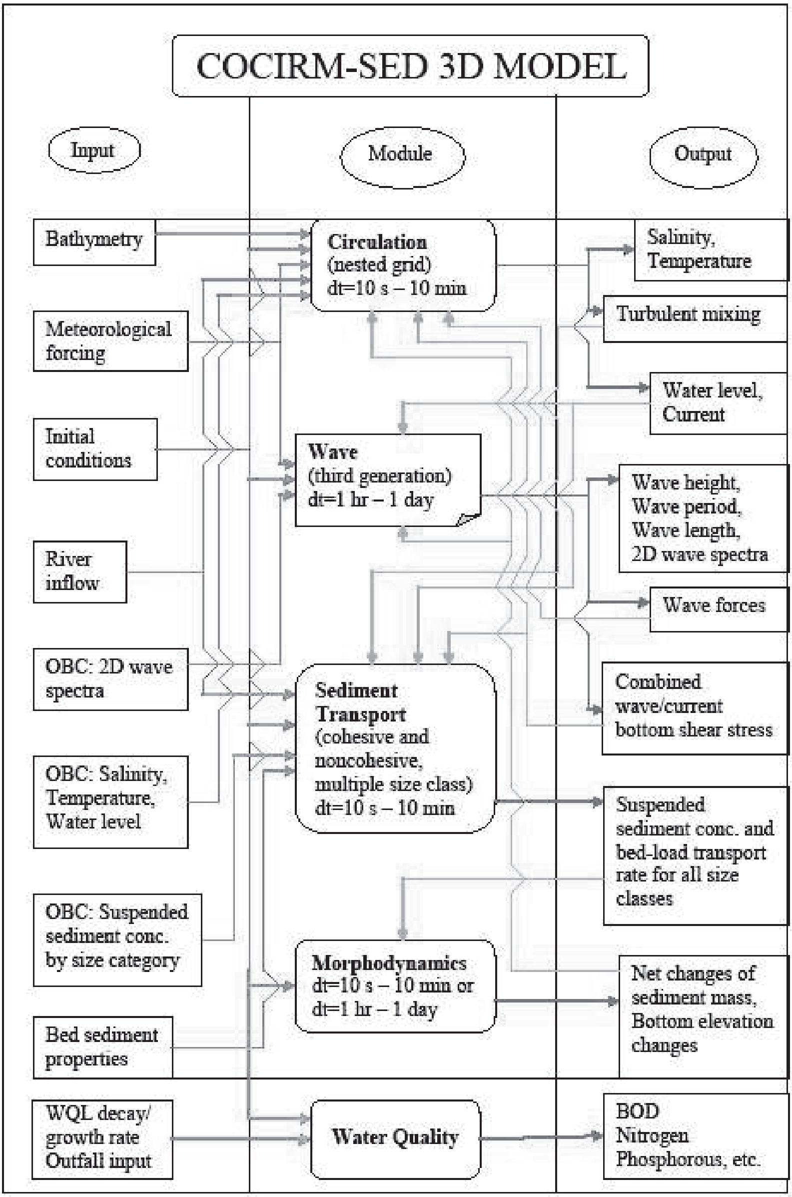

Figure 2. Schematic Diagram of COCIRM-SED system.

For cohesive sediments, bottom deposition, D_k (Krone, 1962), erosion, E_k (Parchure and Mehta, 1985), and settling velocity, w_k (Mehta and Li, 1997) are given by

$$D_k = w_{s,k} c_k S\left[1 - \frac{\tau_{cw}}{\tau_d}\right] \tag{1}$$

$$E_k = f_k M_{\max} \exp(-\chi \tau_e{}^{\lambda}) S[\tau_{cw} - \tau_e] \tag{2}$$

$$w_{s,k} = \left[\frac{a c_k{}^{\alpha}}{(c_k{}^2 + b^2)^{\beta}}\right]\left[\frac{\rho_{s,k} / \rho(\theta,s,c) - 1}{1.65}\right]\left[\frac{10^{-6}}{\upsilon(\theta,c)}\right] F(\theta) \tag{3}$$

where S[-] is a switch function which becomes zero if the quantity inside the square brackets becomes negative, τ_{cw} is the bottom shear stress due to current and wave (Grant and Madsen, 1979), τ_d is the critical shear stress for deposition, τ_e is the critical shear stress for erosion, $M_{\max}$ is the maximum erosion constant at $\tau_{cw} = 2\tau_e$, χ, λ, a, b, α and β are the sediment-dependent empirical coefficients, θ is the temperature, $\rho_{s,k}$ is the sediment granular density of k^{th} sediment, $\rho(\theta,s,c)$ is the temperature, salinity and sediment dependent fluid density, $\upsilon(\theta,c)$ is the temperature and sediment dependent fluid viscosity, and $F(\theta)$ is the temperature effect function on flocculation, $F(\theta)=1.777-0.0518\theta$, for θ=0–30 °C (Jiang, 1999). Two types of cohesive sediment beds are classified, namely newly-deposited and fully-consolidated beds. The newly-deposited bed goes through consolidation process (Toorman and Berlamont, 1993), while the dry weight for the fully-consolidated bed is simply computed using empirical profile formula. The shear strength of the bottom cohesive sediments is then calculated in terms of solid weight fraction.

For non-cohesive sediments, the effect of particle interaction on settling velocities is considered as follows

$$w_k = \left(1 - \frac{c}{\rho_{s,k}}\right)^4 w_{k0} \tag{4}$$

where c is the total suspended sediment concentration, and w_{k0} is the free settling velocity. By assuming spherical particles, the Stokes law is a fairly good approximation of free settling velocity with Reynolds number Re < 0.5 ($\mathrm{Re} = w_{k0} d_k / \upsilon$). For higher Reynolds number, the effects of inertia and virtual mass have to be accounted for. Due to the effect of flow separation behind the falling particle, the value of the drag coefficient depends strongly on the level of free stream turbulence, apart from turbulence caused by the particle itself. In this case, the formulas reported in Rijn (1984a) are applied. Two separated parts are involved in coarse sediment transport, namely suspended-load and bed-load. The formulas introduced in Rijn (2001) are used for calculating the bed-load transport rates. For